

# Corrosion performance of the electroless Ni–P coatings prepared in different conditions and optimized by the Taguchi method

A. Farzaneh · M. Ehteshamzadeh · M. Mohammadi

Received: 13 January 2010/Accepted: 5 September 2010/Published online: 17 September 2010  
© Springer Science+Business Media B.V. 2010

**Abstract** This paper presents an experimental study on the influence of anionic surfactant sodium dodecyl sulfate (SDS), pH, substrate finishing and annealing temperature on the corrosion resistance of electroless nickel phosphorus (Ni–P) coatings using electrochemical techniques and optimization of process parameters based on the Taguchi method. Parameters were selected in three levels and L9 from orthogonal robust array design was used. Corrosion performance of the electroless Ni–P coatings was evaluated by polarization and electrochemical impedance spectroscopy (EIS). Scanning electron microscope (SEM), Energy dispersive X-ray spectroscopy (EDS) and X-ray diffraction (XRD) analysis were used for studying surface morphology and chemical composition of the electroless Ni–P coatings. The results showed that SDS surfactant causes increasing of corrosion resistance and improves surface morphology. Finally, optimum conditions were achieved as, surfactant concentration: 1.5 g L<sup>-1</sup>, pH: 5.5, substrate finishing provided with emery paper no, 2000, and annealing temperature of 200 °C.

---

This paper is dedicated to the memory of the founder of Kerman University, Mr. Alireza Afzalipour, on the occasion of the centenary of his birth and to the memory of his cultured wife, Mrs. Fakhreh Saba.

---

A. Farzaneh · M. Ehteshamzadeh (✉)  
Department of Materials Science and Engineering,  
Faculty of Engineering, Shahid Bahonar University of Kerman,  
Kerman, Iran  
e-mail: ehtesham@mail.uk.ac.ir

A. Farzaneh · M. Ehteshamzadeh · M. Mohammadi  
Department of Materials, International Center for Science,  
High Technology and Environmental Sciences, Kerman, Iran

**Keywords** Electroless Ni–P coating · Surfactant · Taguchi method · EIS

## 1 Introduction

Electroless deposition of the nickel phosphorus alloy coatings (electroless Ni–P) have been widely used in many industrial applications for their unique properties such as corrosion resistance, wear resistance, non-magnetism, improved micro-hardness and coating thickness uniformity [1, 2]. Electroless Ni–P is a barrier coating that protects the substrate by sealing it from the environment. Because of its amorphous nature and passivity, the corrosion resistances of the coatings are excellent and in many environments are superior to that of pure nickel or chromium alloys [3, 4]. It is obvious that increasing of coating porosity decreases the corrosion resistance of the coating. The important factor that affects the coating porosity and ultimate resistance to corrosion attack is surface roughness which is influenced by mechanical preparation of the surface and electroless nickel process procedure [5]. Corrosion resistance of an electroless Ni–P coating is a function of its chemical composition and in particular the phosphorous content. When electroless Ni–P deposits are heated to temperatures upper than 220 °C, nickel phosphide particles begin to form and lead to reduction in the P content of the remaining material. So, the corrosion resistance of these coatings is decreased by such heat treatment [6–8]. Consequently, applications and requirements investigations have been carried out with the aim of improving specific aspects of the product or the process. Recently, some researchers showed that adding surfactant in the bath improves the coating morphology and other properties of the coating [9–11]. Surfactants are surface active agents that lower the surface tension of a liquid,

allowing easier spreading and lower the interfacial tension between two liquids. Surfactants can be classified according to the presence of formally charged groups in their heads. A nonionic surfactant has no charge group in its head and anionic surfactant carries a net charge. If the charge is negative, the surfactant is called anionic; if the charge is positive, it is called cationic [12, 13]. Many attempts have been made to find out the effect of surfactants on the roughness of electroless and electrodeposited Ni–P coatings. However, no report is available on optimization of the process parameters of electroless Ni–P coating to achieve maximum corrosion resistance using anionic surfactant (SDS).

This study deals with the application of the Taguchi method to determine the optimum coating process parameters in order to obtain maximum corrosion resistance. Based on the Taguchi orthogonal experiments were designed with four design parameters, namely, surfactant concentration ( $\text{g L}^{-1}$ ), pH, emery paper number, annealing temperature as independent variables. All of the parameters were selected in three levels as maximum, minimum and middle levels.

## 2 Experimental details

### 2.1 Coating deposition and heat treatment

Mild steel (AISI 1040) specimens of the size  $10 \times 10 \times 6 \text{ mm}^3$  were used as the substrate material for deposition of electroless Ni–P coatings. The samples were then subjected to the surface finishing process. The specimens were polished by successive emery papers (numbers: 120, 500 and 2000). The typical surface finish values ( $\text{Ra}$ ) for each sample, measured using a stylus instrument, are as follows: 0.4, 0.2 and 0.08 for emery papers number of 120, 500 and 2000, respectively. After thorough cleaning, the step-by-step cleaning procedure was employed prior to plating consists of cleaning the substrate with acetone, cleaning in ethanol, acid pickling for 1 min [in  $\text{H}_2\text{SO}_4$ , 8 vol%], followed by immersion in ethanol. Samples were rinsed by double distilled water after each pretreatment stage mentioned. Table 1 lists the electroless bath composition and operating conditions. Electroless Ni–P deposition was

carried out using nickel sulfate as the source of nickel and sodium hypophosphite as the reducing agent and SDS surfactant was used in different concentrations of 0, 0.5 and  $1.5 \text{ g L}^{-1}$ . Elansezhan et al. [14] showed that surfactant in more than  $1.5 \text{ g L}^{-1}$  decreases the hardness of the coating. So, the maximum concentration of the surfactant was chosen  $1.5 \text{ g L}^{-1}$ . Also, pH value of the bath was maintained at a nearly constant value by adding the required quantity of dilute hydrochloric acid and ammonia while being monitored using a pH-meter. The coating thicknesses for all specimens were 18–20  $\mu\text{m}$ . After applying the coating in the bath, the samples were washed in distilled water and ethanol. Finally, the samples were heat treated at one of the three temperatures of 200, 400 and 600 °C under argon atmosphere (annealed for 1 h) according to the experiments design. All chemicals were of analytical reagent grade (Merck).

### 2.2 Design of experiment

Taguchi design can determine the effect of factors on the characteristic properties and the optimal conditions of the factors. This is a simple and systematic approach to optimize design for performance, quality and costs [15]. In Taguchi method, orthogonal arrays and analysis of variance (ANOVA) are used as the tools of analysis. ANOVA estimates the effect of a factor on the characteristic properties and experiment can be performed with the minimum replication using the orthogonal arrays [16, 17]. Based on the Taguchi method, an orthogonal array (OA) was employed to reduce the number of experiments for determining the optimal coating process parameters. L9 OA which has 9 rows corresponding to the number of tests with 4 columns at three levels was chosen. Table 2 lists parameters and its levels used in this study. The response

**Table 2** Variables and their levels

Variable	Level 1	Level 2	Level 3
A: pH	4	4.5	5.5
B: surfactant concentration ( $\text{g L}^{-1}$ )	0	0.5	1.5
C: emery paper no.	120	500	2000
D: annealing temp. (°C)	200	400	600

**Table 1** Electroless bath compositions and operating conditions

Bath compositions		Operating conditions	
Nickel sulphate ( $\text{g L}^{-1}$ )	21	pH	4–5.5
Sodium hypophosphite ( $\text{g L}^{-1}$ )	24	Deposition temp. (°C)	$90 \pm 2$
Lactic acid ( $\text{g L}^{-1}$ )	23	Bath vol. (mL)	250
Picric acid ( $\text{g L}^{-1}$ )	2.2	Annealing temp. (°C)	200–600
SDS ( $\text{g L}^{-1}$ )	0–1.5	Successive emery paper no.	120–2000

variable for accomplishing this study was corrosion current density ( $i_{corr}$ ) as a criterion for corrosion rate. The parameters were optimized with the objective of the maximum corrosion resistance.

### 2.3 Equipment

Surface morphology and composition of the electroless Ni–P coatings was studied by scanning electron microscope (SEM) CamScan MV2300 equipped with energy dispersive X-ray spectroscopy (EDS). X-ray diffraction analysis (Philips X'pert, XRD, Cu  $K\alpha$  radiation) was used for detection of the phases formed in the electroless Ni–P coatings after heat treatment. Surface roughness of the electroless Ni–P deposits was measured using a stylus instrument (MAHR POCKET SURF EMD-1500-311). Electrochemical studies were carried out using potentiostat/Galvanostat model 263A EG&G Princeton Applied Research (PAR) and a classical three electrodes cell with a platinum electrode as counter electrode, saturated calomel electrode (SCE) as reference electrode and the samples with an exposed area of  $1 \text{ cm}^2$  as working electrode. The potentiodynamic polarization curves were recorded using a constant voltage scan rate of  $1 \text{ mV s}^{-1}$ . Electrochemical impedance spectroscopy (EIS) measurements were done in the frequency range of  $100 \text{ kHz}$ – $10 \text{ mHz}$  and the perturbation amplitude was  $5 \text{ mV}$ . Aqueous solution of  $3.5\%$  NaCl was used as the corrosive media in the electrochemical tests. The corrosion parameters values were calculated from polarization and EIS plots [18]. In the polarization curves, the results were analyzed using “Softcorr 352” software by Tafel extrapolation (linear parts of anodic and cathodic branches) of the curves about  $\pm 150 \text{ mV}$  versus OCP. Also, the spectra of EIS were analyzed in terms of an equivalent circuit using “ZView2”. It should be noted that the samples were kept in the electrolyte before recording the polarization curves and impedance spectra for stabilizing.

## 3 Results and discussion

### 3.1 Taguchi array design and analysis of variance

The Taguchi OA design was used to identify the optimal conditions and to find the parameters having the most principal influence on the corrosion rate of the electroless Ni–P coatings. Table 3 shows the structure of the Taguchi's orthogonal array design and the results of the measurements. Table 4 shows contribution of every factor in the response (corrosion rate). According to this table, pH doesn't have any significant contribution effect on the corrosion rate. PH, A, C and D factors were chosen as models parameters which have main significant effect on

**Table 3** L9 OA with design factors and their levels

Std	A	B	C	D	$i_{corr} (\mu\text{A cm}^{-2})$
1	1	1	1	1	0.640
2	1	2	2	2	1.60
3	1	3	3	3	3.90
4	2	1	2	3	2.50
5	2	2	3	1	0.77
6	2	3	1	2	3.70
7	3	1	3	2	0.87
8	3	2	1	3	4.56
9	3	3	2	1	0.54

**Table 4** Contribution of every factor in the response

Term	DOF	Sum of squares	Mean square	Contribution (%)
A–A	2	0.17	0.09	0.83
B–B	2	3.67	1.83	17.90
C–C	2	3.71	1.85	18.10
D–D	2	12.95	6.47	63.18

**Table 5** Analysis of variance (ANOVA)

Term	Sum of squares	DOF	Mean square	F value	p Value prob > F
Source model	20.32	6	3.39	39.75	0.0247
B–B	3.67	2	1.83	21.52	0.0444
C–C	3.71	2	1.85	21.76	0.0439
D–D	12.95	2	6.47	75.97	0.0130
Residual	0.17	2	0.09		

the response. The variance of the corrosion rate was calculated (analysis of variance) and the results were listed in Table 5. According to Table 5 ( $p$  value) selected model and its parameters are significant in the 90% confidence interval. In addition, it shows that on the basis of the present analysis, D (annealing temperature), C (Emery paper no.) and A (surfactant concentration) are the most effective parameters on the corrosion rate ( $i_{corr}$ ) of electroless Ni–P coatings. All the calculations were performed using Design expert 7.0. Figure 1 shows correlation between predicted and actual results of the corrosion rate having R square equals to 99.17%. That confirms that the fitted model to the results is acceptable.

### 3.2 Determination of the optimal conditions using Taguchi method

In this research, Taguchi method was used to optimize the parameters in order to achieve to the best corrosion resistance. By optimizing of the model using Design expert 7.0

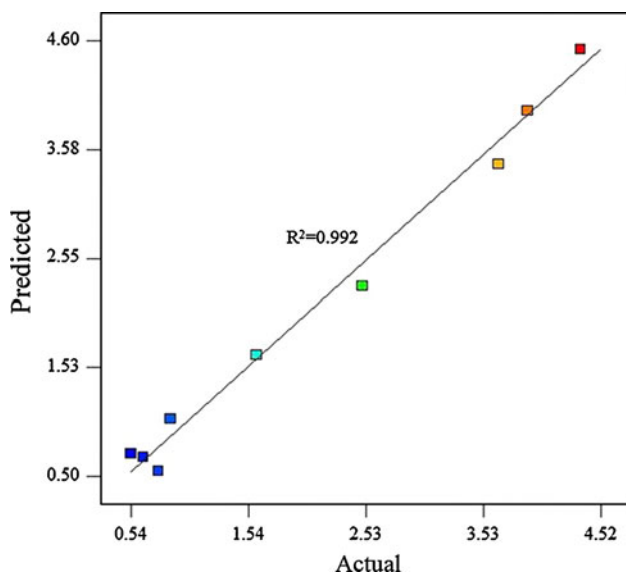


**Fig. 1** Correlation between predicted and actual results of the coatings corrosion current density according to the L9 OA designed factors listed in Table 3

**Table 6** Optimum conditions and performance

Factors	Level desc.	Level
Surfactant con. ( $\text{g L}^{-1}$ )	1.5	3
pH	5.5	3
Emery paper no.	2000	3
Annealing temp. ( $^{\circ}\text{C}$ )	200	1
Estimated result for corrosion current density	0.29 ( $\mu\text{A cm}^{-2}$ )	

software, optimum conditions were achieved as listed in Table 6. According to the model prediction, minimum corrosion current density was  $0.29 \mu\text{A cm}^{-2}$  and belonged to the coating precipitated in the condition and therefore

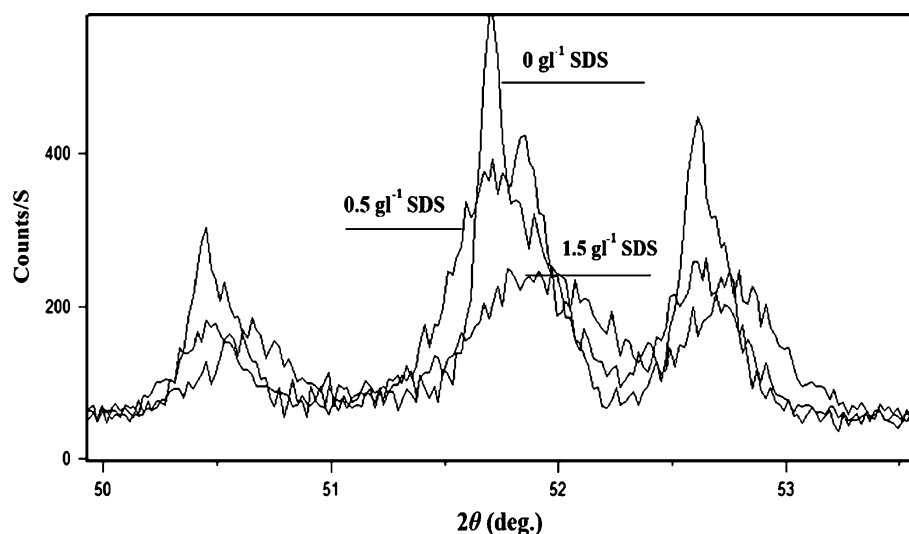
optimum condition as: surfactant concentration =  $1.5 \text{ g L}^{-1}$ , pH = 5.5, emery paper number = 2,000 and annealing temperature =  $200^{\circ}\text{C}$ .

### 3.3 Surface morphology and corrosion performance of the electroless Ni–P deposits

#### 3.3.1 Surface morphology and composition

Diffraction patterns of the electroless Ni–P deposits prepared in various concentrations of SDS was shown in Fig. 2. It is obvious that adding the surfactant causes broadening of the peaks. Adding surfactant to the bath decreases crystal size of the electroless Ni–P coatings. Some researchers showed that in the absence of surfactant, the electroless Ni–P deposits are purely crystalline and in the presence of SDS, the coating structure is changed to a mixture of nano-crystalline and amorphous structure and therefore microhardness of deposits increases [14, 19]. In the present study, a similar trend was observed. The typical surface finish values ( $R_a$ ) for each sample were as follows: 0.4, 0.2 and 0.08 for emery papers number of 120, 500 and 2000, respectively. Variation of average roughness values with the number of experimental run in various conditions are presented in Fig. 3. In the recent research, authors showed that in the coatings applied without surfactant, dispersion of nickel particle is less homogeneous than those of applied in the presence of surfactant which results in a uniform surface finish [20]. In this case, surface morphology, roughness and dispersion of nickel particles are improved and are more homogeneous than those obtained under the other conditions. This is due to the fact that at higher concentration of SDS the contact angle is reduced and this leads to the better wettability of electroless Ni–P deposits. It is apparent that SDS addition during

**Fig. 2** XRD patterns of the electroless Ni–P coatings deposited in the presence of different concentrations of SDS surfactant



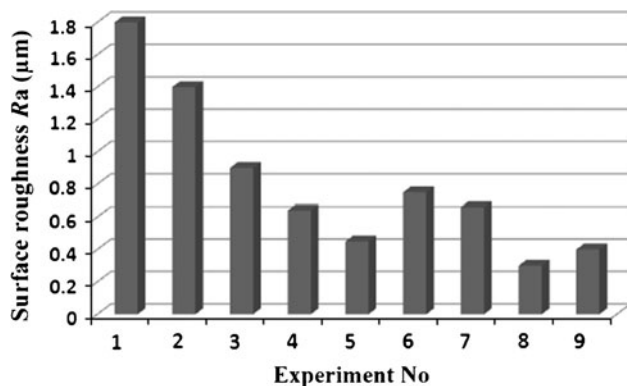


**Fig. 3** Average surface roughness of the electroless Ni–P deposits in different conditions shown as the experiment number

electroless Ni–P deposition can improve the coating roughness.

### 3.3.2 Potentiodynamic polarization studies

Typical polarization curves of the electroless Ni–P coatings precipitated in different conditions (listed in Table 3) are shown in Fig. 4. Corrosion parameters obtained for each sample are given in Table 7. Results for the mild steel substrate are also included in Table 7. Although there are peaks on the some anodic branches of these curves and a

**Table 7** Polarization parameters of mild steel and the electroless Ni–P coatings in 3.5% NaCl according to the L9 OA designed factors listed in Table 3

Std	$E_{corr}$ (mV)	$i_{corr}$ ( $\mu\text{A cm}^{-2}$ )	Std	$E_{corr}$ (mV)	$i_{corr}$ ( $\mu\text{A cm}^{-2}$ )
1	-350	0.540	6	-505	3.70
2	-445	1.60	7	-446	0.87
3	-503	3.90	8	-274	4.50
4	-485	2.50	9	-479	0.64
5	-333	0.77	Mild steel	-700	20

decrease in the current density showing passivity to some extent, this passivity is not persistent and is broken with a little increasing in oxidizing power of the environment. So, Tafel extrapolation (linear parts of anodic and cathodic branches) of the curves about  $\pm 150$  mV versus OCP was used in “Softcorr 352” software for determination of corrosion current density.

Polarization results indicate that addition of SDS surfactant to the coating bath leads to decrease in corrosion rate of electroless Ni–P coatings. In the presence of the surfactant, crystalline grain size of the coating microstructure was decreased [21]. This may be interpreted as Ni particles produced inside the electrolyte deposit on the substrate surface and surfactant addition does not allow the

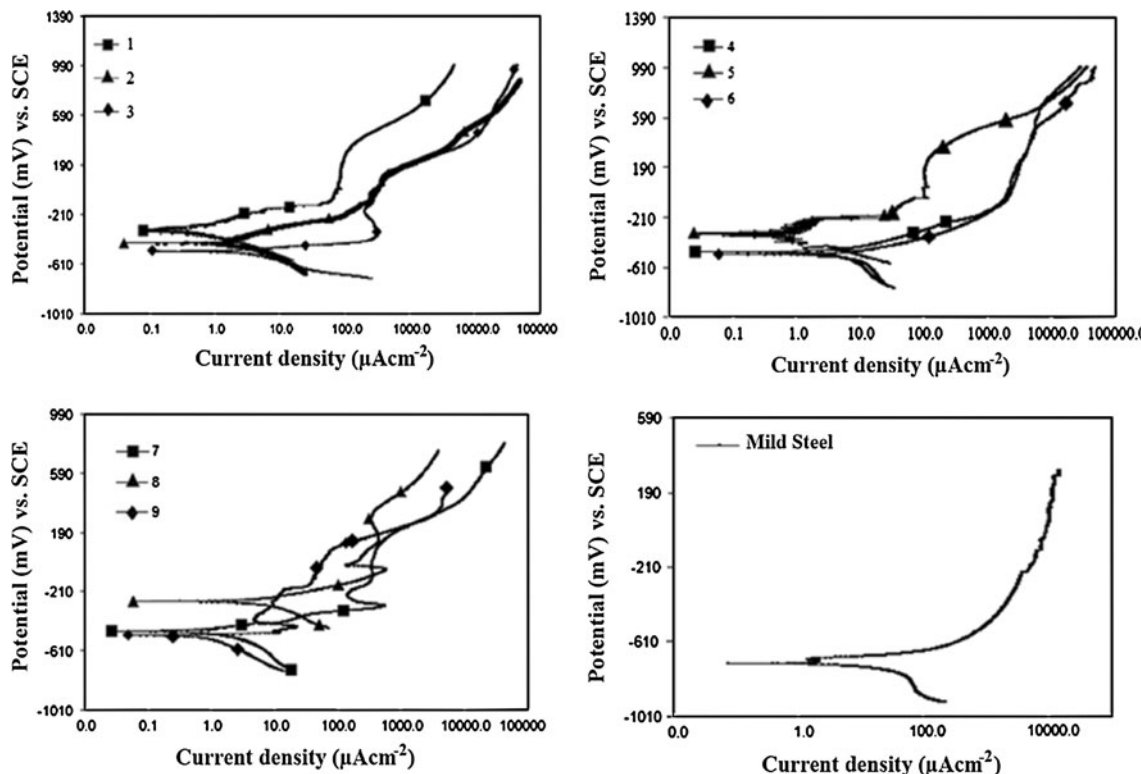


**Fig. 4** Polarization curves of mild steel and the electroless Ni–P coatings in 3.5% NaCl according to the L9 OA designed factors listed in Table 3

Ni particles to escape to the top surface and get deposited in the regions other than the substrate surface, therefore it have been causes decreasing of porosity in final deposit and increasing of its corrosion resistance as a final result.

The electroless Ni–P coatings which heat treated at 200 °C showed amorphous microstructure. Amorphous alloys exhibit better corrosion resistance than equivalent polycrystalline materials, because of the absence of grain or phase boundaries and because of the glassy films which form on the surface to make it passive [21]. Furthermore, in amorphous state, the surface passive film is covered by a layer of adsorbed hypophosphite/phosphinate species which act as a protective layer. The large variation in the cathodic Tafel slope in these coatings can be attributed to the surface inhibition by a passive film. By increasing annealing temperature up to 400 °C, the microstructure of the coating is converted from amorphous to crystalline state. Heat treatment at the temperature 400 °C to achieve maximum hardness lowers the corrosion resistance of the electroless Ni–P coating, probably as a result of micro-cracking and phase transformation. It has been reported that semi-coherent Ni<sub>3</sub>P phases are created approximately at 400 °C and consequently microhardness increases whereas the size of Ni<sub>3</sub>P precipitates increases. By increasing temperature to 600 °C these phases changed from semi-coherent to non-coherent state [22]. When temperature increases, intergranular corrosion in NaCl solution will be more probable owing to the growth of the microcrystallites. This fact is further supported by the observed corrosion results (Table 7). EDS results indicate that by adding surfactant, phosphorus content of the coatings increases from 9% up to 12 wt%. Increasing phosphorus content of the electroless Ni–P coating results in higher amount of Ni<sub>3</sub>P compound. It is may be the reason for improving corrosion performance at the presence of surfactant. When surfactant added, Ni<sub>3</sub>P sited in deposit by nanostructure form and decreases the porosity of coating. Roughness of the substrate clearly has a substantial and systematic effect on the corrosion behavior of coatings. Grinding produces a thin (about 1.0 μm), hard, white layer, on the machined surface which is in residual compression (about 600 MPa) and resists corrosion. Tomlinson et al. [23] suggested that the white layer on the ground specimen is the cause of decreasing in the corrosion current that might have been expected on the basis of the roughness. Increasing pH accelerates deposition rate and causes improvement in the surfactant effect and microstructure became finer, but in the presence of surfactant the effect of pH on corrosion rate cannot be evaluated. Therefore, this parameter is not effective in the Taguchi analyzing. The differences in  $E_{corr}$  of these coatings may be due to the differences in porosity, surface roughnesses and compositions of the coatings. The observed experimental results

such as dependence of structure and corrosion resistance on the plating conditions, increase in crystalline nature of the coating with heat treatment and dependence of chemical reactivity of coatings with composition on the amorphous state are in conformity with the other investigations [24, 25].

### 3.3.3 Electrochemical impedance spectroscopy studies

Figure 5 shows the Nyquist and Bode plots of electroless Ni–P coatings precipitated in various conditions. The polarization resistance ( $R_p$ ) value is inversely proportional to the corrosion rate of the system. This parameter provides an estimation of the protective efficiency of the coating. Also, Bode plots demonstrate that only one time constant is observed for the electrochemical system under study. The equivalent circuit shown in Fig. 6 was used for modeling of the coating corrosion property parameters, where  $R_s$  is resistance of the solution,  $R_c$  is the passive coating resistance and CPE is the constant phase element which is mainly used to explain the system heterogeneity and some distribution of the value of physical properties of the system [26, 27]. The impedance expression of CPE is defined by:

$$Z_{CPE} = \frac{1}{A(j\omega)^n} \quad (1)$$

where  $A$  and  $n$  are frequency-independent fit parameters,  $j = (-1)^{1/2}$  and  $\omega = (2\pi f)$  is the angular frequency. The factor  $n$ , defined as CPE power, is an adjustable parameter that lies between 0.5 and 1 and is defined as the roughness factor in Eq. 2 [28–31]:

$$n = \frac{A}{A_0} \quad (2)$$

where  $A$  and  $A_0$  are the apparent and real surface areas, respectively. As  $n$  approaches unity, the corrosion current density becomes smaller and capacitive essence of the CPE goes toward ideality. It is notable that  $n$  is dimensionless.

Constant phase element (CPE) is substituted for capacitances and reflects the deviation of the capacitance behavior from ideality. In the modeling step, two fractions was adjusted for a CPE that were CPE-T (which reflects capacitive essence of it) and CPE-P (which reflects its deviation from ideality) that is the same  $n$ .

The fitted results of electroless Ni–P coatings are listed in Table 8. The EIS results also demonstrate that the corrosion resistances of electroless Ni–P coated samples are several times greater than that of the AISI 1040 steel substrate. According to one of the most convincing models proposed to explain the high corrosion resistance of electroless Ni–P coatings, preferential dissolution of nickel occurs even at the open circuit potential and leads to the

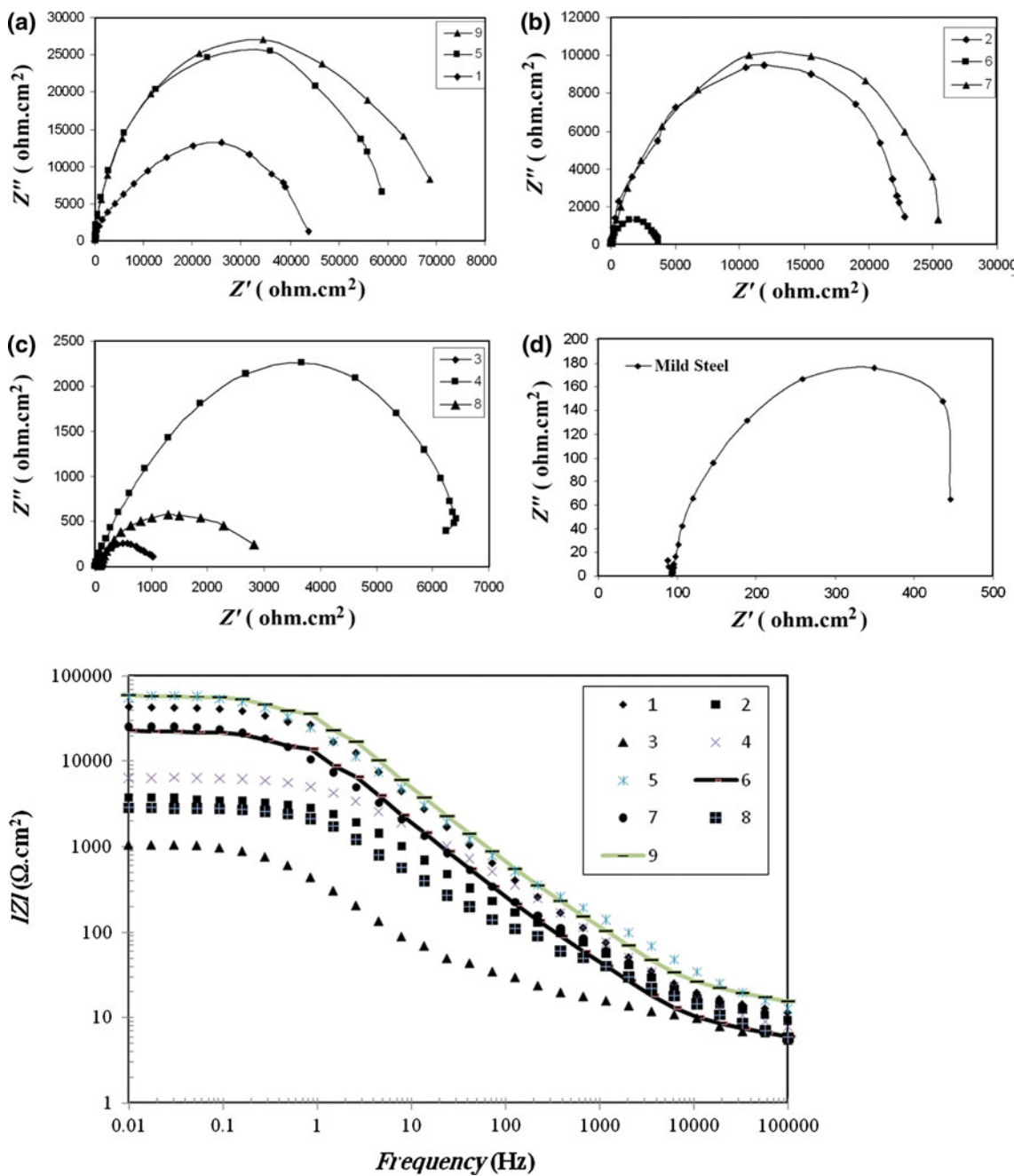


**Fig. 5** The Nyquist and Bode plots of the electroless Ni-P coatings in 3.5% NaCl electrolyte; annealed at **a** 200 °C; **b** 400 °C; **c** 600 °C and **d** mild steel

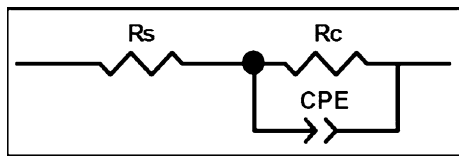


**Fig. 6** Schematic of equivalent circuit for modeling the impedance spectra of the electroless Ni-P coatings

phosphorus enrichment of the surface layer. The enriched phosphorus surface reacts with water to form a layer of adsorbed hypophosphite anions. This layer in turn will block the supply of water to the electrode surface, thereby prevents the hydration of nickel, which is considered to be the first step to form either soluble  $\text{Ni}^{2+}$  species or a passive nickel film [32, 33]. The coating corrosion resistances,

**Table 8** Impedance parameters of mild steel and the electroless Ni–P coatings in 3.5% NaCl according to the L9 OA designed factors listed in Table 3

Std	R <sub>S</sub> (ohm cm <sup>2</sup> )	R <sub>C</sub> (ohm cm <sup>2</sup> )	CPE-P ( <i>n</i> )	CPE-T (μF)	Standard errors (%)
1	5.33	28381	0.79776	38.54	5.5
2	6.381	26280	0.8355	16.15	4.2
3	9.614	812.6	0.64543	257.13	5.3
4	6.446	6553	0.72001	23.39	6
5	5.136	58003	0.93063	20.87	4.6
6	8.049	5186	0.6391	74.83	4.2
7	4.775	17372	0.72836	77.75	4.8
8	10.06	2335	0.62005	56.339	5
9	72.53	65552	0.93395	21.66	4
Mild steel	92.49	446	0.85883	285.02	4

R<sub>C</sub>, increased and the capacitive component of the constant phase elements (CPE) decreased in different range, meaning that the coating structures changed to a denser and more homogenous film after heat-treatment at 200 °C and in the presence of SDS. By comparing the corrosion resistances of the electroless Ni–P coatings obtained in various conditions listed in Table 3 it is seen that the latter coating (condition in experiment 9) appeared to offer better protection against corrosion in 3.5% NaCl media. This effect can be ascribed to a reduction in the porosity and grain boundary available for corrosion in electroless Ni–P coating. In the optimal condition (Table 6) that was obtained by Taguchi method, the ratio of apparent surface area to real surface area (*n*) reaches approximately as high as 0.93 (std = 9 in Table 8) which posses the maximum coating resistance (R<sub>c</sub> = 65552) and so, the minimum corrosion current density in the minimum real surface area. So, the results of Fig. 3 are in a very good agreement with the results of Table 8. In Table 3 the condition of experiment number 9 is the nearest condition to the optimal condition (A3B3C3D1 in Table 3 or the surfactant concentration = 1.5 g L<sup>-1</sup>, pH = 5.5, emery paper number = 2,000 and annealing temperature = 200 °C) and in Fig. 3 this experiment number has one of the lowest surface roughness and in Table 8, the coating prepared in the condition of experiment number 9 has the highest corrosion resistance.

A clear distinction can be made between the samples without SDS (3) and with SDS (9) coatings on the basis of their respective CPE-T values. The coating number 9 shows consistently lower CPE-T value (<30 μF) than the coating number 3 (>250 μF). So, it can be said that SDS reduces porosity of the deposition.

#### 4 Conclusion

Taguchi orthogonal array was employed to optimize surfactant concentration and other parameters to reach the

maximum corrosion resistance of the electroless Ni–P coatings. Based on the experimental results and analysis, the following conclusions can be drawn which clearly indicate that there is possibility of a significant improvement in the corrosion resistance of electroless Ni–P deposited layers.

- (1) Annealing temperature, surfactant concentration and substrate finishing procedure have significant influences on the corrosion resistance of the electroless Ni–P coatings.
- (2) Heat-treatment at 400 and 600 °C crystalize the amorphous structure of electroless Ni–P coatings and decrease its corrosion resistance.
- (3) Corrosion tests performed that electroless Ni–P coatings deposited in all conditions significantly improve the corrosion resistance of mild steel.
- (4) The optimal condition of depositing the electroless Ni–P coating to achieve the minimum corrosion rate was obtained as: the surfactant concentration = 1.5 g L<sup>-1</sup>, pH = 5.5, emery paper number = 2,000 and annealing temperature = 200 °C.

**Acknowledgments** Funding support for this work was provided by Vice Chancellor Research of International Center for Science, High Technology and Environmental Sciences according to the research project number 618801 in the period of 2009/2010 and is highly acknowledged. The authors would like to acknowledge Mr. Javad Vazifeh Mehrabani for his help in analysis of results.

#### References

1. Hamdy AS, Shoeib MA, Abdel Salam OF (2007) Surf Coat Technol 20:162
2. Davis JR Associates (2001) Surface engineering for corrosion and wear resistance. ASM International, Cleveland, OH
3. Riedel W (1991) Electroless nickel plating. Finishing Publications Ltd, Stevenage, Hertfordshire, UK
4. Baudrand DW (1994) Electroless nickel plating. Surface engineering. ASM International, Cleveland, OH
5. Kerr C, Barker D, Walsh F (1997) Trans Inst Met Finish 75:81

6. Gavrilov GG (1979) Chemical (electroless) nickel plating. Portcullis Press, UK
7. Bielinski J, Krolkowski A, Kedzierska I et al (1995) Model Chem 132:685
8. Rajam KS, Rajagopal I, Rajagopalan SR (1990) Plat Surf Finish 77:63
9. Malfatti CF, Veit HM, Menezes TL et al (2007) Surf Coat Technol 201:6318
10. Shukla N, Ahner J, Weller D (2004) J Magn Magn Mater 1349:272
11. Lin YC, Duh JG (2006) J Alloys Compd 439:74
12. Myers D (2006) Surfactants science and technology. Wiley, Hoboken, NJ
13. Tadros FT (2005) Applied surfactants, principles and applications. Wiley-VCH, Berkshire
14. Elansezhan R, Ramamoorthy B, Kesavan Nair P (2008) Surf Coat Technol 203:709
15. Cox DR, Reid N (2000) Theory of the design of experiments. Chapman and Hall/CRC, Boca Raton, FL, USA
16. Roy R (1990) A primer on the Taguchi method. Van Nostrand Reinhold, New York
17. Park SH (1996) Robust design and analysis for quality engineering. Chapman and Hall, London, UK
18. Stansbury E, Buchanan R (1998) Fundamentals of electrochemical corrosion. ASM International, Materials Park, OH, p 248
19. Elansezhan R, Ramamoorthy B, Kesavan Nair P (2009) J Mater Process Technol 209:233
20. Mallory GO, Hajdu JB (eds) (1999) Electroless plating: fundamental and applications. AESF, Orlando, FL
21. Farzaneh A, Ehteshamzadeh M, Ghorbani M, Vazifeh Mehrabani J (2010) J Coat Technol Res 7:547
22. Alirezaei Sh, Monirvaghefi SM, Salehi M et al (2004) Surf Coat Technol 184:170
23. Tomlinson WJ, Carroll MW (1990) J Mater Sci 25:4972
24. Mimani T, Mayanna SM (1996) Surf Coat Technol 79:246
25. Crobu M, Scorcipino A, Elsener B et al (2008) Electrochim Acta 53:3364
26. Chang YY, Wang DY (2005) Surf Coat Technol 200:2187
27. Balaraju JN, Sankara Narayanan TSN, Seshadri SK (2001) J Solid State Electrochem 5:334
28. Ehteshamzadeh M, Shahabi T, Hosseini MG (2006) Appl Surf Sci 252:2949
29. Zheludkovich ML, Sera R, Montemor MF, Miranda Salvado IM, Ferreira MGS (2005) Electrochim Acta 51:208
30. Lamaka SV, Zheludkovich ML, Yasakau KA, Montemor MF, Ferreira MGS (2007) Electrochim Acta 52:7231
31. Wang H, Akid R (2007) Corros Sci 49:4491
32. Diegle RB, Sorensen NR, Clayton CR et al (1988) J Electrochem Soc 135:1085
33. Carbalal J, White E (1988) J Electrochem Soc 135:2952